Journal of ELECTRONIC MATERIALS, Vol. 45, No. 9, 2016
DOI: 10.1007/s11664-016-4633-z
© 2016 The Minerals, Metals & Materials Society (outside the USA)

High-Temperature Characteristics of an InAsSb/AlAsSb n^+Bn Detector

DAVID Z. TING,[1,3] ALEXANDER SOIBEL,[1,2] LINDA HÖGLUND,[1,2] CORY J. HILL,[1,2] SAM A. KEO,[1,2] ANITA FISHER,[1,2] and SARATH D. GUNAPALA[1,2]

1.—Center for Infrared Photodetectors, NASA Jet Propulsion Laboratory, M/S302-231,4800 Oak Grove Drive, Pasadena, CA 91109-8099, USA. 2.—California Institute of Technology, Pasadena, CA 91109, USA. 3.—e-mail: David.Z.Ting@jpl.nasa.gov

The high-temperature characteristics of a mid-wavelength infrared (MWIR) detector based on the Maimon-Wicks InAsSb/AlAsSb nBn architecture was analyzed. The dark current characteristics are examined in reference to recent minority carrier lifetime results. The difference between the responsivity and absorption quantum efficiency (QE) at shorter wavelengths is clarified in terms of preferential absorption of higher-energy photons in the top contact layer, which cannot provide reverse-bias photo-response due to the AlAsSb electron blocking layer and strong recombination. Although the QE does not degrade when the operating temperature increases to 325 K, the turn-on bias becomes larger at higher temperatures. This behavior was originally attributed to the change in the valence band alignment between the absorber and top contact layers caused by the shift in Fermi level with temperature. In this work, we demonstrated the inadequacy of the original description, and offer a more likely explanation based on temperature-dependent band-bending effects.

Key words: Infrared detector, unipolar barrier, nBn, mid-wavelength infrared

INTRODUCTION

The nBn photodetector architecture proposed by Maimon and Wicks[1] provides an effective means for lowering generation-recombination (G-R) dark current by suppressing Shockley–Read–Hall (SRH) processes, and for reducing surface leakage dark current.[1–3] This has been especially beneficial for III–V semiconductor-based infrared photodiodes, which traditionally tend to suffer from excess depletion dark current and a lack of good surface passivation. Recently, Soibel et al. analyzed the high-temperature characteristics of a mid-wavelength infrared (MWIR) detector based on the Maimon–Wicks InAsSb/AlAsSb nBn design, and found that the quantum efficiency (QE) does not degrade when the operating temperature increases to above room temperature.[4] It was also found that the turn-on bias becomes larger at higher temperatures. This behavior was originally attributed to the change in the valence band (VB) alignment between the absorber and top contact layers caused by the shift in Fermi level with temperature. In this work we provide additional analysis that demonstrates the inadequacy of the original description, and offer a more plausible explanation based on temperature-dependent band-bending effects. We also provide clarification on basic device dark current and quantum efficiency characteristics.

BASIC DEVICE CHARACTERISTICS

The InAsSb/AlAsSb nBn structure consisting of a 700 Å InAsSb top contact layer, a 300 Å InAsSb spacer layer, a 1000 Å AlAsSb electron barrier, and a 2-μm-thick InAsSb absorber lattice-matched to the GaSb substrate; the alloy compositions are $InAs_{0.915}Sb_{0.085}$

(Received October 22, 2015; accepted May 5, 2016; published online May 20, 2016)

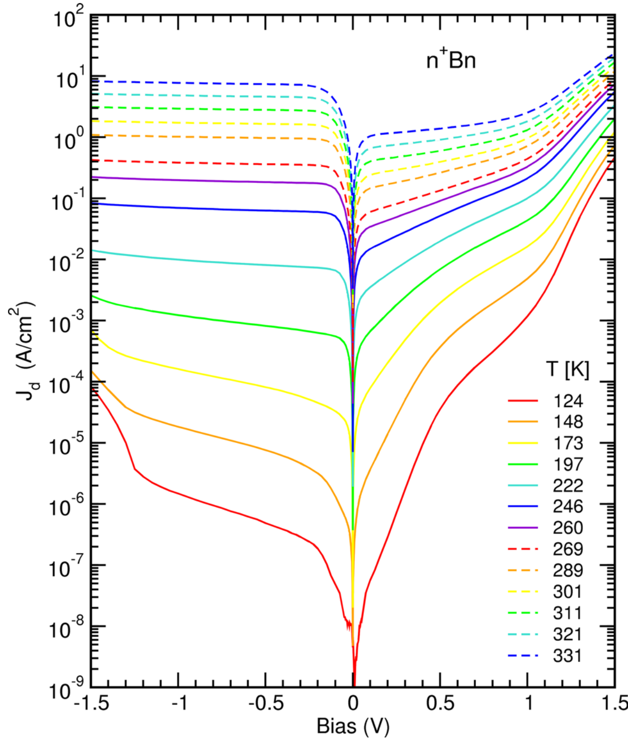

Fig. 1. Dark current density–voltage characteristics for an nBn device at temperatures ranging from 124–331 K.

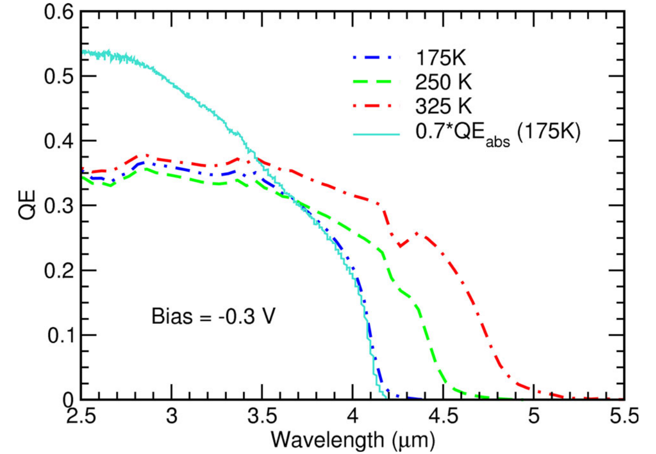

Fig. 2. The spectral quantum efficiency (QE) for an nBn structure taken under −0.3 V bias at 175 K, 250 K, and 325 K. The 175 K absorption quantum efficiency (QE_{abs}), multiplied by transmission factor 0.7, is also included for comparison.

and $AlAs_{0.9}Sb_{0.1}$. The nominal doping density of the top contact layer is $N_c = 6 \times 10^{17}$ cm^{-3}. The spacer, barrier, and absorber layers are not intentionally doped. The absorber layer background doping level extracted from capacitance–voltage measurement is $N_\alpha \sim 1–2 \times 10^{15}$ cm^{-3},[5] and estimated residual doping level in the barrier is $P_B \sim 1 \times 10^{15}$ cm^{-3}. Detailed description of the device structure and performance has been reported elsewhere;[4] here, we summarize and clarify some of the key device results before focusing on the high-temperature turn-on behavior in the next section. Figure 1 shows the dark current density–voltage (J-V) characteristics of the device at temperatures ranging from 124 K to 331 K. Arrhenius analysis indicates diffusion-limited behavior down to ~170 K, with an activation energy of 0.34 eV, which is close to the value of E_g (T = 0) = 0.33 eV. Below 170 K, generation-recombination (G-R) dark current dominates, with an activation of 0.18 eV, which is slightly larger than $E_g/2$. In the diffusion-limited temperature range, the dark current level is approximate 30 times the value given by the Rule'07.[6,7] To determine the generation rate in the quasi-neutral absorber region, we found through optical modulation response (OMR) measurement that the minority carrier lifetime remains fairly constant at between 300 and 400 ns from 77 to 200 K, and then decreases to 160 ns at 298 K;[5] SRH is the dominating recombination mechanism in the entire temperature range studied. Therefore, we believe the diffusion-limited dark current in the 170–300 K range is primarily determined by SRH generation.

Figure 2 shows the front-side illuminated spectral response QE (QE_{resp}) of a non-anti-reflected coated device measured at 175, 250, and 325 K. The band gap temperature dependence is found to be described by the Varshni expression $E_g(T) = E_{g,0} - \alpha T^2/(T + \beta)$, with $E_{g,0} = 0.33$ eV, $\alpha = 4 \times 10^{-4}$ eV/K, and $\beta = 310$ K.[4] We also measured the absorption QE (QE_{abs}) by taking the ratio of the transmission through the device sample and that of the substrate. The 175 K internal QE_{abs} is adjusted (by multiplying by 0.7 to remove surface reflection effect) for comparison with the external QE_{resp} in Fig. 2. The (external) QE_{resp} agrees well with the reflection-adjusted (internal) QE_{abs} for wavelength $\lambda > 3.6$ μm. However, QE_{resp} flattens out for $\lambda < 3.6$ μm, while the QE_{abs} continues to increase as λ decreases. This difference may be explained by looking at the absorption in the heavily doped top contact. In a reverse (negatively) biased nBn structure, absorption in the (front-side illuminated) top contact layer does not contribute to the photo-response because the photo-excited carriers are confined in the contact layer (electrons are blocked by the barrier "B", and they in turn hold back the holes electrostatically) where they recombine readily in the heavily doped region or at the surface. A higher fraction of the shorter wavelength photons are absorbed in the top contact layers due to a higher absorption coefficient. In addition, degenerate doping band filling in the top contact layer significantly reduces the absorption of (longer-wavelength) photons with energy close to the band gap. For T = 175 K and $N_c = 6 \times 10^{17}$ cm^{-3}, the difference between the Fermi level and the conduction band edge is $(E_F - E_c) = 0.081$ eV, which is

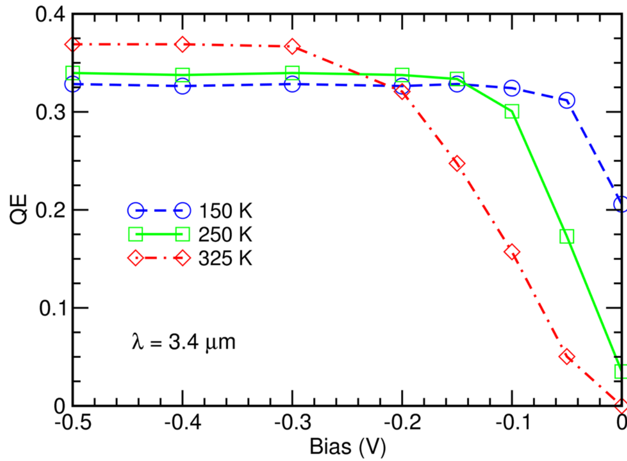

Fig. 3. QE measured at $\lambda = 3.4$ μm as functions of bias for an nBn structure taken under −0.3 V bias at 150, 250, and 325 K.

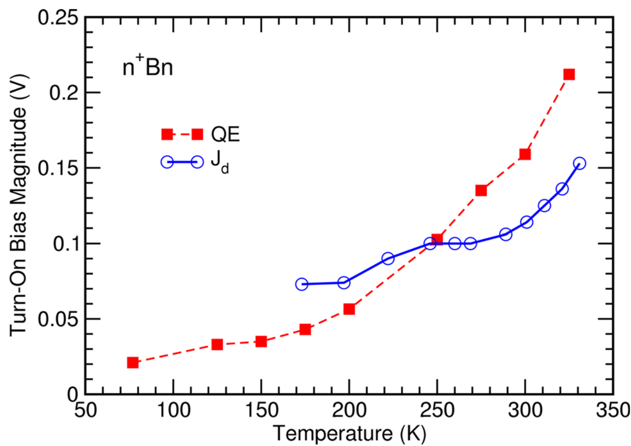

Fig. 4. QE and dark current turn-on bias as functions of temperature.

significant when compared to band gap $E_g = 0.313$ eV. As a result, longer wavelength photons can transmit more readily through the top contact layer into the absorber to contribute to the photo-response; hence, we find good agreement between QE_{resp} and QE_{abs} for wavelength $\lambda > 3.6$ μm.

HIGH-TEMPERATURE TURN-ON CHARACTERISTICS

Figure 3 shows QE measured at $\lambda = 3.4$ μm as a function of applied bias for $T = 150$, 250, and 325 K. We observe that the magnitude of the QE turn-on bias (defined as the bias at which QE reached 90% of the plateau value) increases with increasing temperature. Figure 4 shows the magnitudes of the QE turn-on bias and the dark current turn-on bias (define as the knee position in the reverse-bias J-V curve) as functions of temperature; both show an increase with temperature. This behavior is somewhat surprising since we normally would expect the turn-on bias to decrease with increasing temperature, as thermionic emission over a minority blocking energy barrier would become more efficient.

An explanation proposed in Ref. 4 is illustrated in Fig. 5 with schematic low- and high-temperature energy band diagrams. In both cases, the degenerate n-doping in the top contact layer forces the valence band edge (E_v) to be lower than that in the low-doped absorber, creating an energy barrier ΔE_v for the minority carriers (holes). The hole barrier ΔE_v becomes larger at higher temperatures as the Fermi level in the absorber approaches the intrinsic Fermi level and moves towards the mid-gap. Overcoming the larger ΔE_v would in turn require a higher applied bias. While plausible, this explanation is shown to be inadequate upon more careful examination of doping and temperature dependence of the Fermi level.

Figure 6 shows the calculated electron and hole carrier densities, and Fermi levels as functions temperature for $InAs_{0.91}Sb_{0.09}$ with various n-type doping levels. Numerical density of states (DOS) is used in our calculations to account for the effect of conduction band (CB) non-parabolicity. Because the CB DOS is much smaller than VB DOS, the intrinsic Fermi level is closer to E_c than E_v, especially at higher temperatures as E_g decreases. At higher doping levels, the quantity $(E_F - E_v)$, which determines the hole barrier ΔE_v, decreases monotonically with temperature. At lower doping levels $(E_F - E_v)$ becomes non-monotonic; it decreases with temperature initially, but then

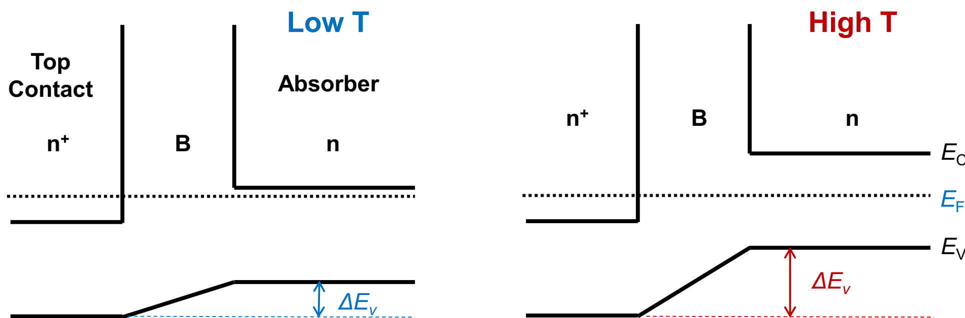

Fig. 5. Schematic energy band diagrams for the n⁺Bn structure at low and high temperatures.

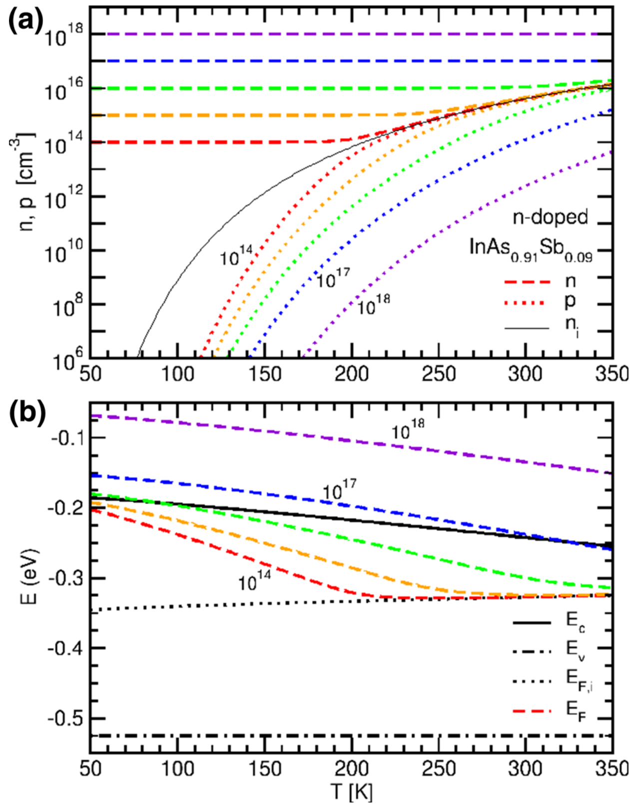

Fig. 6. Calculated electron and hole carrier densities (a), and Fermi levels (b) as functions temperature for $InAs_{0.91}Sb_{0.09}$ with *n*-type doping levels of 10^{14} cm^{-3}, 10^{15} cm^{-3}, 10^{16} cm^{-3}, 10^{17} cm^{-3}, 10^{18} cm^{-3}. The intrinsic carrier density is shown as the solid line in (a). The intrinsic Fermi level and the conduction and valence band edges are respectively shown as dotted, solid, and dash-dot black lines in (b).

increases once the temperature is sufficiently high for intrinsic carrier densities to dominate. Figure 7 shows the zero-bias energy band diagrams near the electron barrier at 150 and 350 K for the InAsSb/AlAsSb n^+Bnn^+ structure calculated using a one-dimensional heterojunction drift–diffusion model.[8] The model structure includes a highly doped n^+ bottom contact layer to reduce minority carrier injection. With the numerically calculated Fermi levels, we observe that the low temperature hole barrier $\Delta E_v(150\ K) = 0.119$ eV is only marginally smaller than the high temperature barrier $\Delta E_v(350\ K) = 0.134$ eV. In fact, at 200 K the hole barrier $\Delta E_v(200\ K) = 0.137$ eV is actually slightly larger than that at 350 K. Therefore, the original argument from Ref. 4 attributing the greater turn-on bias at higher temperature to larger hole barrier ΔE_v cannot be correct, especially when considering that relative k_BT, ΔE_v is actually smaller at higher temperature.

To explore the possible cause of the larger turn-on bias at higher temperature we examine the energy band diagrams and carrier concentrations of the model n^+Bnn^+ device structure under various reverse biases at 150 K in Fig. 8 and at 350 K in Fig. 9. The modeling results lead us to an alternative explanation based on temperature-dependent band-bending effects. The hole-blocking barrier ΔE_v can be overcome more effectively if the applied bias is dropped over the AlAsSb electron barrier region and vicinity (as intended in the nBn design). Comparing 150 K and 350 K simulation results, we note that at zero bias the 350 K carrier densities ($n = 1.73 \times 10^{16}\ cm^{-3}$; $p = 1.53 \times 10^{16}\ cm^{-3}$) in the absorber region are intrinsic, with the majority carrier density being approximately one order of magnitude higher than the extrinsic level. The zero-bias carrier densities are extrinsic at 150 K ($n = 2 \times 10^{15}\ cm^{-3}$; $p = 1.52 \times 10^{9}\ cm^{-3}$). It can also be seen in Fig. 7 that under zero bias, for both 150 K and 350 K the absorber region immediately to the right of the barrier is accumulated due to band bending; accumulation is stronger in the 350 K case because at higher temperature the band

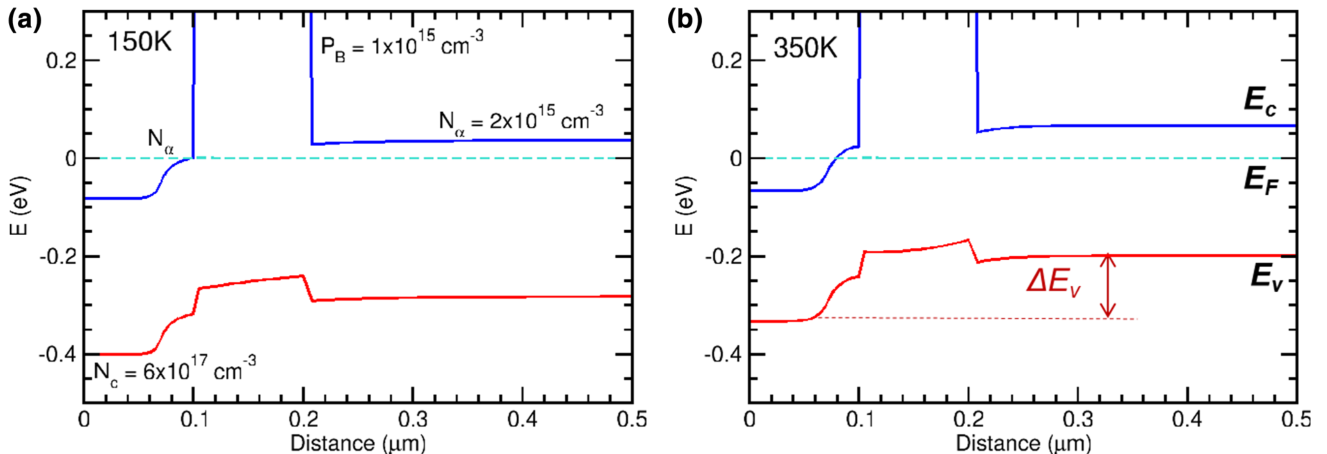

Fig. 7. Calculated zero-bias energy band diagrams for the n^+Bnn^+ structure at (a) 150 K, and (b) 350 K. The doping levels for the top contact, spacer, barrier, absorber, and bottom contact layers are respectively $N_c = 6 \times 10^{17}\ cm^{-3}$, $N_s = 2 \times 10^{15}\ cm^{-3}$, $P_B = 1 \times 10^{15}\ cm^{-3}$, $N_\alpha = 2 \times 10^{15}\ cm^{-3}$, and $N_{bc} = 2 \times 10^{17}\ cm^{-3}$.

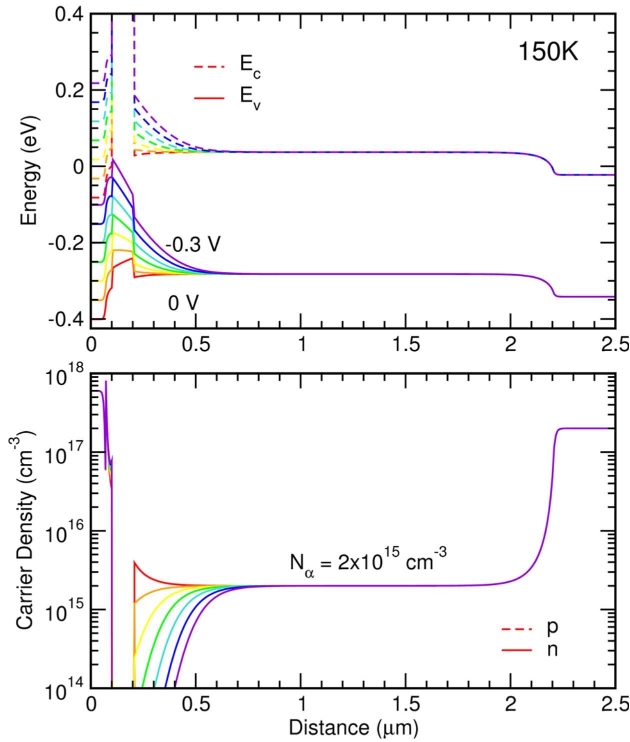

Fig. 8. Calculated 150 K energy band diagrams and electron carrier density (n) for the n^+Bnn^+ structure under 0 V to −0.30 V applied bias at 0.05 V intervals. Hole carrier density levels (p) are too low to be seen in the figure.

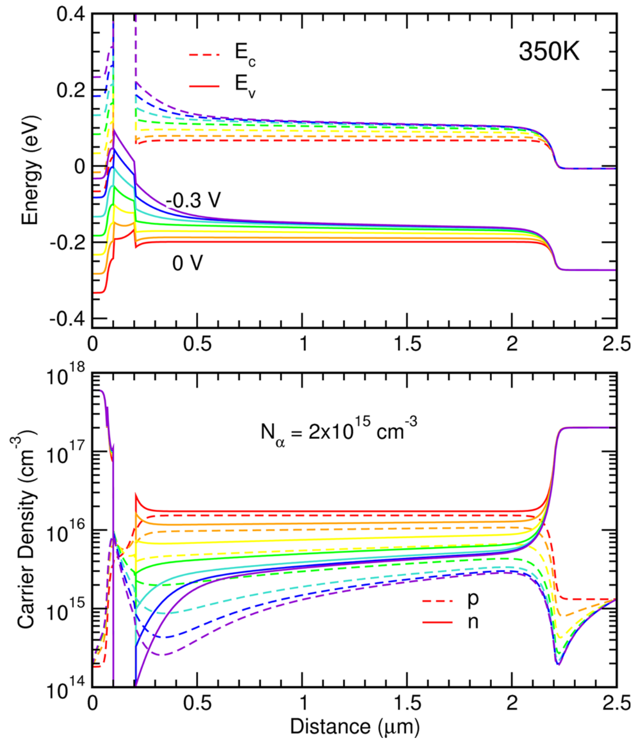

Fig. 9. Calculated 350 K energy band diagrams and electron (n) and hole (p) carrier densities for the n^+Bnn^+ structure under 0 V to −0.30 V applied bias at 0.05 V intervals.

edges of the slightly p-type barrier are brought down more as the barrier Fermi level moves up towards the barrier mid gap. At 150 K, the applied reverse bias acts entirely on the electron barrier and vicinity, and serves to increase the depletion width in the absorber region to the right of the barrier. At 350 K, the bias drops not only in the electron barrier and nearby regions, but also over the n–n^+ junction between the absorber and the bottom contact. This can be seen in Fig. 10, which shows the electric field distribution at 150 K and 350 K under the same biasing conditions. The applied bias serves not only to deplete the absorber region to the right of the barrier, but also to extract carrier in excess of the extrinsic levels from the absorber region. At 350 K, the depletion width increases more slowly with applied bias. Under −0.1 V the region to the right of the barrier is still slightly accumulated at 350 K, but is depleted at 150 K. It appears that at higher temperatures a smaller fraction of the bias drop goes towards overcoming the hole-blocking barrier ΔE_v because of the much higher carrier densities in the absorber layer. This effect also appears to be reflected in the dark current characteristics, which is depletion-current dominated at below 170 K (see Fig. 8 for absorber depletion next to the AlAsSb electron barrier under bias), and diffusion-limited at above 170 K.[4]

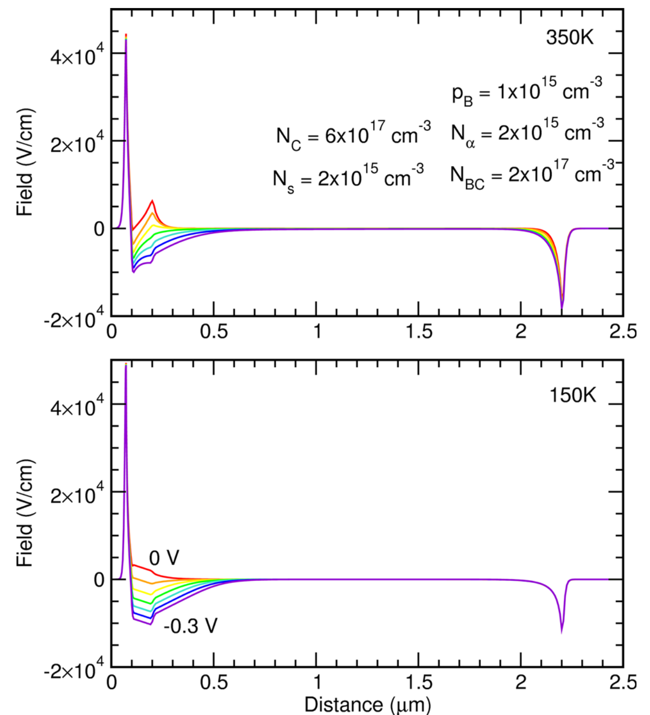

Fig. 10. Calculated electric field distribution at 150 K and 350 K for the n^+Bnn^+ structure under 0 V to −0.30 V applied bias at 0.05 V intervals.

SUMMARY

We re-examine the results on the high-temperature characteristics of a mid-wavelength infrared (MWIR) detector[4] based on the Maimon–Wicks InAsSb/AlAsSb nBn design.[1] The dark current characteristics are analyzed in reference to recent minority carrier lifetime results.[5] The difference between the responsivity and absorption QE at shorter wavelengths is clarified in terms of preferential absorption of higher energy photons in the top contact layer, which cannot provide any reverse-bias photo-response due to the AlAsSb electron blocking layer and high recombination. It had been observed that although the QE does not degrade when the operating temperature increases to above room temperature, the turn-on bias becomes noticeably larger.[4] This counter-intuitive behavior was originally attributed to the change in the band alignment between the absorber and top contact layers caused by the shift of the absorber and the heavily-doped contact layer band edges relative to the Fermi energy, thereby forming a larger hole-blocking barrier at higher temperatures. We provide additional analysis that demonstrates the inadequacy of the original argument, and show that at higher temperatures more applied bias is required to overcome the hole-blocking barrier, as it is more difficult to deplete the regions in the vicinity of the AlAsSb barrier due to high intrinsic carrier density levels.

ACKNOWLEDGEMENTS

We thank R. Rosenberg and R. Kowalczyk for technical assistance. The research described in this publication was carried out at the Jet Propulsion Laboratory, California Institute of Technology, under a contract with the National Aeronautics and Space Administration.

REFERENCES

1. S. Maimon and G.W. Wicks, *Appl. Phys. Lett.* 89, 151109 (2006).
2. G.W. Wicks, G.R. Savich, J.R. Pedrazzani, and S. Maimon, *Proc. SPIE* 7608, 760822 (2010).
3. G.R. Savich, J.R. Pedrazzani, D.E. Sidor, S. Maimon, and G.W. Wicks, *Appl. Phys. Lett.* 99, 121112 (2011).
4. A. Soibel, C.J. Hill, S.A. Keo, L. Höglund, R. Rosenberg, R. Kowalczyk, A. Khoshakhlagh, A. Fisher, D.Z.-Y. Ting, and S.D. Gunapala, *Appl. Phys. Lett*. 105, 023512 (2014).
5. L. Höglund, D.Z.-Y. Ting, A. Soibel, C.J. Hill, A.M. Fisher, S.A. Keo, and S.D. Gunapala, *IEEE Photonics Technol. Lett.* 27, 2492 (2015).
6. W.E. Tennant, D. Lee, M. Zandian, E. Piquette, and M. Carmody, *J. Electron. Mater.* 37, 1406 (2008).
7. W.E. Tennant, *J. Electron. Mater.* 39, 1030 (2010).
8. E.S. Daniel, X. Cartoixa, W.R. Frensley, D.Z.-Y. Ting, and T.C. McGill, *IEEE Trans. Electron. Devices* 47, 1052 (2000).